Novel recombination mechanism for interacting bound-exciton complexes in Cu-doped ZnTe

P. O. Holtz
Department of Physics and Measurement Technology, Materials Science Division, Linköping University, S-581 83 Linköping, Sweden

B. Monemar
Department of Physics and Measurement Technology, Materials Science Division, Linköping University, S-581 83 Linköping, Sweden and Département de Recherche Fondamentale, Section de Physique du Solide, Centre d'Etudes Nucléaire de Grenoble, 85X, 38041 Grenoble Cedex, France

H. P. Gislason
Department of Physics and Measurement Technology, Materials Science Division, Linköping University, S-581 83 Linköping, Sweden

Ch. Uihlein and P. L. Liu
Max Planck Hochfeld-Magnetlabor Grenoble, 166X, 38042 Grenoble Cedex, France
(Received 25 February 1985)

A novel recombination mechanism is observed for excitons bound at Cu-related complex centers in highly doped ZnTe. In addition to each principal bound-exciton (BE) line, sharp peaks corresponding to new satellite transitions are observed towards lower energies in photoluminescence and resonant Raman scattering. Such satellites are observed to be related to principal excitons bound at acceptors as well as isoelectronic centers. The novel spectral features are displaced from the associated principal BE's by energies that correspond to electronic excitations of different acceptors. An interaction with nearby acceptors, at which a final-state excitation occurs, gives rise to the observed "transfer" processes. Part of the recombination energy is then transferred to the nearby acceptor in the recombination event, causing a corresponding reduction in the emitted photon energy. This is different from ordinary two-hole transitions, where the final-state excitation occurs at the same acceptor at which the exciton is bound. This novel recombination mechanism will be denoted as two-hole transfer transitions. The Zeeman spectra for the satellite lines reflect the magnetic behavior of the initial as well as the final state. This gives rise to a large number of components in the Zeeman spectra for the satellites, differing from the corresponding spectra for the principal BE state.

I. INTRODUCTION

The ability of defects in semiconductors to bind more than one charge carrier in a localized potential, i.e., bound-exciton (BE) excitations, has been recognized for more than two decades.[1] The electronic structure of such bound excitons for simple defects, such as substitutional impurities in the host lattice, has been investigated extensively by optical spectroscopy, as recently reviewed by Dean and Herbert.[2] The understanding of more complex defects such as the association of two or more atoms is less advanced, although some progress in the understanding of electronic properties of such defects has recently been made in a few rather well-defined systems.[3]

Low doping levels usually favor simple substitutional defects. Such defects may bind excitons, which yield well-defined discrete lines usually dominating the optical spectra. Photoluminescence (PL) and absorption spectra give detailed information on the electronic structure of these defects. The recombination of bound-exciton excitations can be described as independent local events, even though the BE wave functions may be quite extended. Such recombination processes have been studied in great detail both for excitons bound at neutral isoelectronic defects as well as donors and acceptors in more common semiconductor materials.[2] In many cases a detailed picture of the electronic energy levels for both the BE state as a whole and the individual particles in the complex has been achieved from optical spectroscopy.[3–5] In the case of excitons bound at donors or acceptors, information on energy levels for the ground state of the BE system, i.e., for the defect binding of the exciton, can be obtained from so-called two-particle spectra.[2,6] Recently, such two-hole spectra in ZnTe have given the energies of up to seven *s*-like excited states of the simple acceptors Cu_{Zn} and Ag_{Zn}.[7]

With increasing doping level the formation of associations involving two or more dopant atoms becomes more probable in comparison with simple substitutional defects. New BE lines appear in optical spectra usually displaced towards lower photon energies compared to the simple substitutional acceptor BE spectra close to the band edge. Such BE states associated with acceptors or donors as well

as isoelectronic defects can be observed in optical experiments in contrast to electrical measurements, where transitions involving the latter group are not readily detectable. The rich structure normally observed in such BE spectra gives valuable information for the identification of these defect associates, which are formed via defect reactions at high doping levels.

This study presents a novel recombination mechanism which occurs at Cu-related complex defects in highly doped ZnTe. The details of the defect complexes, at which this type of recombination is observed, will be described separately.[8] Therefore only a brief account of the general features of optical spectra related to strong Cu doping in ZnTe will be given in this paper. Instead, we shall mainly concentrate on the new recombination mechanism, which gives rise to novel spectral features observed in photoluminescence and resonant Raman scattering (RRS). These spectral features of electronic origin are displaced from the respective associated principal BE lines towards lower energies by an amount approximately corresponding to an unperturbed $1s$-$2s$ excitation of a shallow acceptor different from the defect the exciton is bound at. Thus at high doping levels the BE recombination at complex associations interacts strongly with nearby neutral acceptor states, causing a final-state excitation of this acceptor as a result of the BE recombination. This interaction mechanism, which we shall denote "two-hole transfer transitions" (THTT), is to be understood as a generalization of ordinary two-hole transitions with more than one defect site involved in the BE recombination process.

This paper is organized in the following way. In Sec. II the details of material preparation and doping are briefly described, together with a description of the experimental setup used in the optical spectroscopy. Section III contains the experimental data from several types of optical experiments, including PL, RRS, PL excitation (PLE), optical transmission, and magneto-optical Zeeman measurements. In Sec. IV we discuss briefly the schematic theoretical formalism for the THT and THTT spectra as well as some specific general aspects in relation to the data presented in Sec. III. Finally, Sec. V summarizes the main conclusions from this work.

II. SAMPLE PREPARATION AND EXPERIMENTAL PROCEDURE

The ZnTe material used for this investigation was grown by B. Schaub [Laboratoire d'Electronique et de Technologie Informatique (LETI), Grenoble] with a modified Bridgman technique from Te solution. Single-crystalline samples of a size typically $5\times5\times1$ mm^3 were cut from larger polycrystalline slices. A thin Cu layer was evaporated on the polished and etched (2% bromine-methanol solution, 3 min) samples. The subsequent diffusion was made in an open N_2-flow system at controlled temperatures varying from 250 °C to 650 °C. A typical diffusion time was 1 h. The samples were cooled down slowly in the furnace to avoid severe structural defect formation, e.g., dislocations during rapid cooling. After this diffusion step the remaining Cu layer was polished off, and the samples were etched a second time in the same solution as above. This single-step doping procedure was sufficient to produce a high concentration of complex Cu-related defects in ZnTe, as previously reported.[8] Several different optical experiments were performed, each requiring a specific experimental setup. For the transmission experiments, an ordinary tungsten lamp was used and the transmitted light was recorded through a 0.75-m Jarrell-Ash double-grating monochromator. This monochromator was also used for detection of the laser-excited PL measurements, where an Ar^+ laser was normally employed as an excitation source. Excitation for the selective photoluminescence (SPL) measurements and RRS was achieved with the addition of a cw dye laser. The same setup was used for PLE measurements, where the dye-laser wavelength could be continuously scanned with a stepping-motor arrangement. Sample temperatures could be regulated from 1.8 K to room temperature in an exchange-gas He cryostat.

For the magneto-optical Zeeman data a 10-T superconducting magnet at the Max Planck Hochfeld-Magnetlabor in Grenoble was used in the Voigt configuration. Both PL and simple transmission measurements were performed in this setup. A high-resolution Jobin-Yvon THR 1.5-m double-grating monochromator was available to detect optical spectra at high magnetic fields.

III. OPTICAL SPECTROSCOPY ON BE STATES AT Cu-RELATED DEFECTS IN ZnTe

A. General properties of the transfer transitions

As already mentioned in the Introduction, the formation of Cu-related defect complexes depends critically on the doping level as illustrated in Fig. 1. The different doping concentrations for the PL spectra shown in Fig. 1 were created by choosing different temperatures for these Cu diffusions (for 1 h). At low doping levels the BE line associated with the Cu_{Zn} substitutional acceptor dominates by far the spectrum together with its LO-phonon replicas and two-hole spectra at lower energies. At higher doping levels, on the other hand, a large number of novel BE lines are observed. Actually, more than 20 excitons bound at different defects can be distinguished at high Cu doping. They all occur at lower photon energies; in fact, some electronic BE lines are as deep as 2.03 eV. As will be shown separately, most of these excitons are bound at either complex acceptors or neutral isoelectronic complexes, all involving Cu.[8]

In this paper a limited number of these BE states will illustrate the novel recombination mechanism occurring at high doping levels. These BE states with electronic lines labeled Z_1^0–Z_5^0 are shown in Fig. 1, where additional sharp lines, e.g., Z_1' and Z_1'', can be observed at lower energies (below 2.26 eV). At first sight these sharp lines appear to be separate electronic BE lines related to specific complex defects. A detailed investigation shows, however, that this assumption is not right. One piece of evidence against an ordinary BE state is provided in Fig. 2, where transmission spectra for the same samples as used in PL (Fig. 1) are shown. Clearly the two lines at 2.2507 eV (Z_1') and 2.2176 eV (Z_1'') have no counterpart in absorption, i.e., they appear to be satellite lines rather than

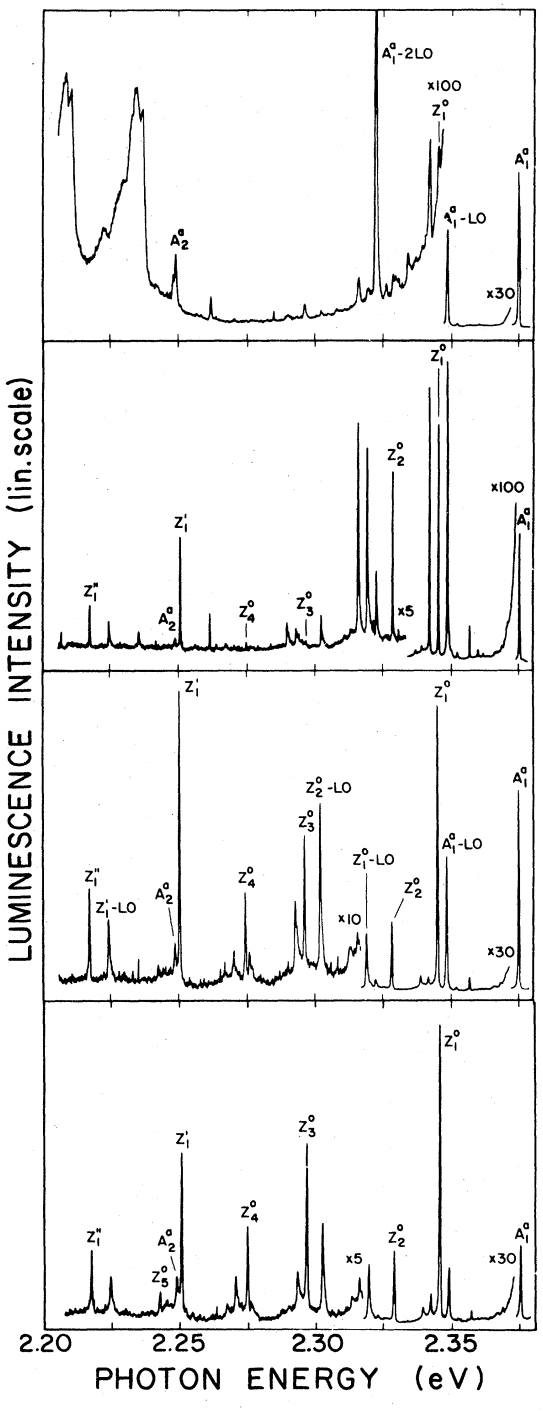

FIG. 1. Photoluminescence (PL) spectra for some ZnTe samples, which have been Cu doped at different diffusion temperatures: 250°C (topmost), 350°C, 450°C, and 550°C, respectively. In low-temperature-diffused samples, the Cu_{Zn} ABE (A_1^a) dominates the spectrum, while in samples doped at higher temperatures deeper Cu-related complexes increase in intensity. The no-phonon lines of the investigated centers at which the transfer processes occur are denoted Z_1^0–Z_5^0 in the figure, while Z_1' and Z_1'' are satellite lines to Z_1^0.

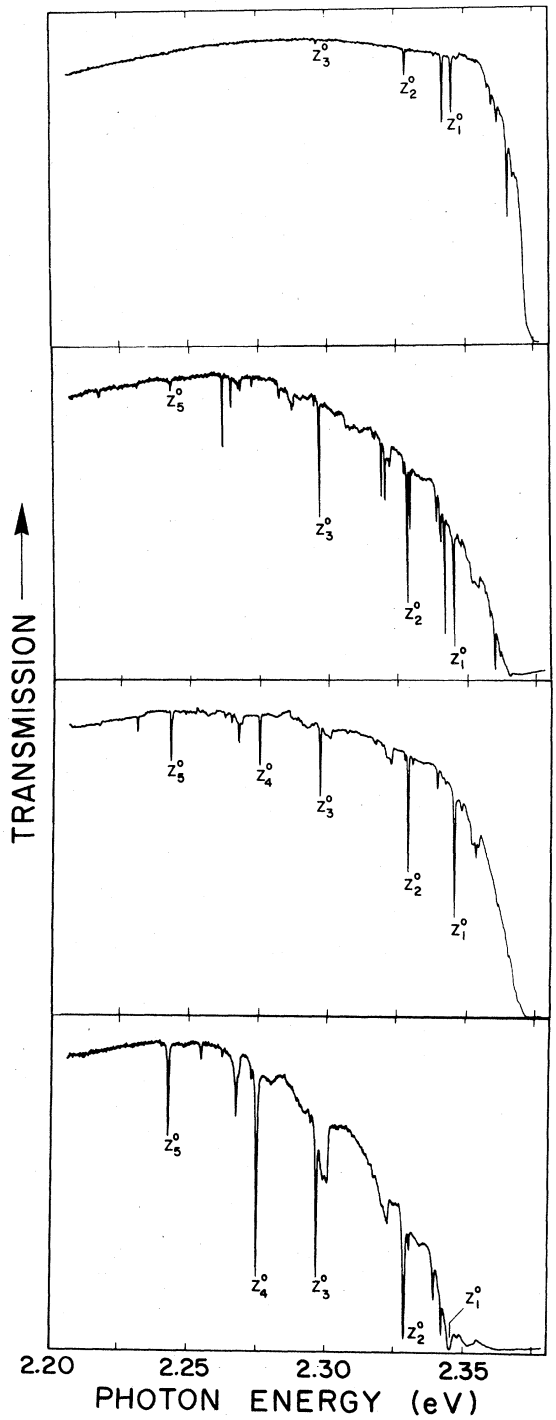

FIG. 2. Transmission spectra for the same ZnTe samples as used for the PL spectra in Fig. 1, Cu-doped at the diffusion temperatures 250°C (topmost), 350°C, 450°C, and 550°C, respectively. The increased intensity ratio for deeper centers relative to more shallow ones with increasing Cu concentration is obvious from these spectra. All no-phonon lines Z_1^0–Z_5^0 observed in the PL spectra are detected also in these transmission spectra, while the satellite lines Z_1' and Z_1'' (Fig. 1) have no counterpart in transmission.

real BE excitations. This picture is further supported by dye-laser-excited PLE spectra with detection at Z_1' and Z_1'', respectively, and also just above these energies. As observed in Fig. 3, the PLE spectra for these two states are identical with the PLE spectrum obtained for the higher-energy BE state Z_1^0 (at 2.3452 eV). Since the Z_1^0 state appears in the direct PLE spectrum obtained by detection in the phonon wing of Z_1^0 (Fig. 3), it can be concluded that Z_1^0 is a real state. This is in contrast to Z_1' and Z_1'', where no resonance was observed at detection in the phonon replicas of these lines. Z_1' was not detected in the PLE spectrum with detection in Z_1'' either. From these facts we can conclude that neither Z_1' nor Z_1'' correspond to real states. The identification of Z_1' and Z_1'' as satellites to the Z_1^0 BE is further supported by the SPL spectra shown in Fig. 4. When the dye-laser excitation is resonant with the Z_1^0 BE state, the transitions Z_1' and Z_1'' are enhanced with very little background from the surrounding spectra. For an excitation at slightly lower energy, on the other hand, no trace of the states Z_1' and Z_1'' can be found (with the exception of a weak RRS component, as described below), in agreement with the PLE spectra in Fig. 3.

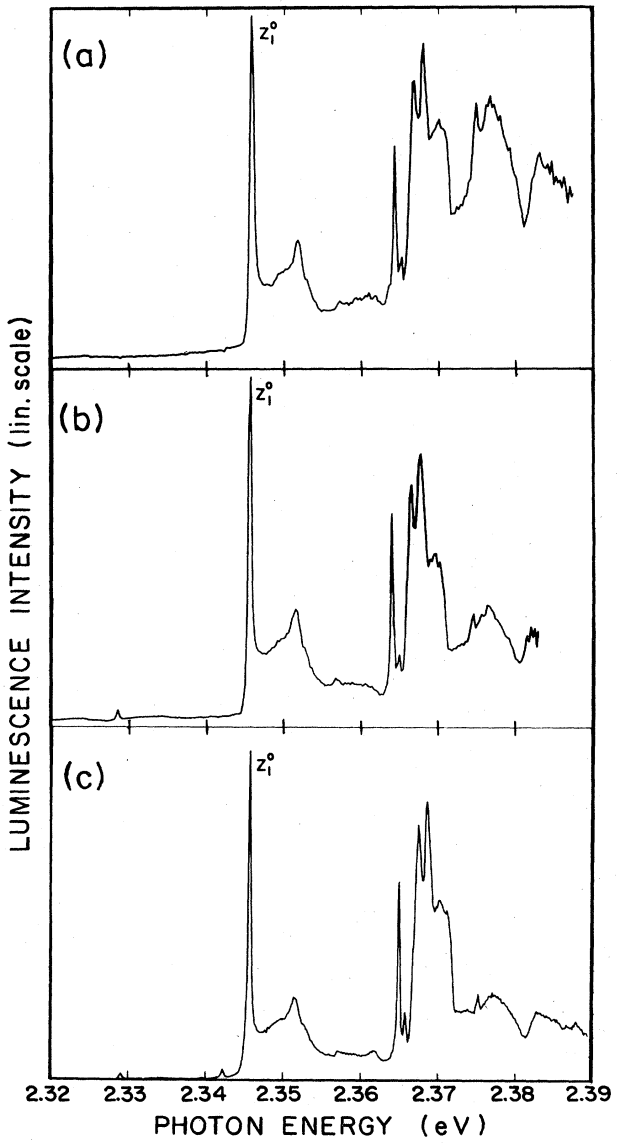

FIG. 3. Photoluminescence excitation (PLE) spectra for the Z_1^0 emission obtained by tunable dye-laser excitation with three different detection wavelengths: (a) Z_1'', (b) Z_1', and (c) the LO replica of Z_1^0. These PLE spectra are almost identical, proving that the lines Z_1' and Z_1'' are related to Z_1^0. When detecting the phonon replicas of Z_1' or Z_1'', no trace of these lines can be observed, when the excitation energy is scanned in the region close to Z_1' and Z_1''. The structure in the range 2.35–2.37 eV is the one-phonon band coupling to Z_1^0, while the peak at 2.375 eV is the Cu_{Zn} ABE.

Obviously Z_1' and Z_1'' do not correspond to real excitations, but are undoubtedly connected with the recombination of the Z_1^0 BE. Evidently there exists some mechanism whereby the Z_1^0 BE recombination energy can be partly transferred to a low-energy excitation, while the rest is radiated as a lower-energy photon, giving rise to Z_1' and Z_1'' in PL (Fig. 1). The energies transferred to the lower-energy excitation are, in this particular case, $h\nu(Z_1^0)-h\nu(Z_1')=94.5$ meV and $h\nu(Z_1^0)-h\nu(Z_1'')=127.6$ meV, respectively. These energies are apparently much too high to correspond to phonon excitations ($LO_\Gamma=26.1$ meV in ZnTe). We therefore conclude that these excitation energies correspond to electronic excitations, which is also reasonable considering the narrow linewidths involved (about 0.3–0.5 meV for Z_1' and Z_1'', depending on the doping level). The general appearance of these satellites resembles the ordinary two-particle spectra observed at low doping levels. Such spectra are due to final-state excitations of the acceptor hole (donor electron) at the BE recombination. As is well known, and is also apparent from Fig. 1, such two-particle spectra

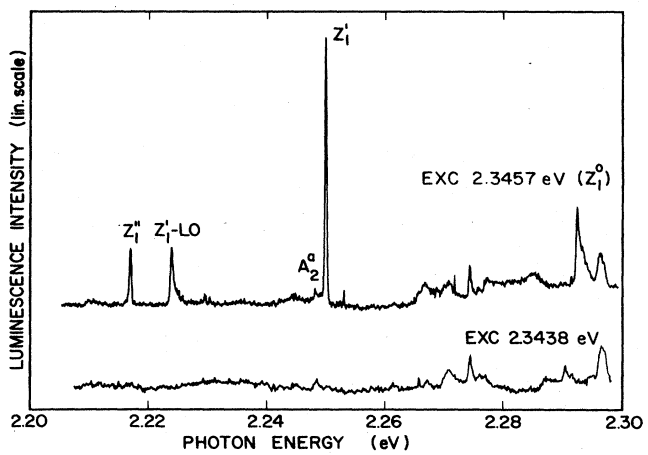

FIG. 4. Portion of the PL spectrum at selective excitation resonant with Z_1^0 (upper curve) and just below Z_1^0 (lower curve). No trace of Z_1' or Z_1'' can be observed when the excitation energy is below Z_1^0 (except for a weak RRS component as demonstrated in Figs. 11 and 12), which further proves that Z_1' and Z_1'' are not real states, but instead satellite lines associated with Z_1^0.

disappear at high doping levels, while the satellite spectra represented by Z_1' and Z_1'' apparently do not.

It has been shown by magneto-optical experiments that Z_1^0 is an exciton bound to an isoelectronic defect complex.[8] This is evident from a simple comparison of the thermalization behavior in transmission and PL at 10 T, as is illustrated in Fig. 5. Thermalization occurs to some degree in PL emission, but not at all in absorption. This proves that the ground state of the Z_1^0 BE system contains no spin (i.e., no particle), and therefore must belong to a neutral isoelectronic center. Further details of magneto-optical data will be discussed in a separate paper.[8]

Clearly such an isoelectronic defect BE cannot give rise to final-state excitations at the center itself, since there is no available particle to be excited in the final state (i.e., the ground state of the BE excitation). Therefore an interaction with a nearby acceptor, at which a final-state excitation occurs, is necessary in the recombination event. Figure 6 shows a schematic illustration of this model. The corresponding case of an acceptor-bound-exciton (ABE) recombination with a final-state excitation is also sketched. As will be shown below, such cases are also observed experimentally. This novel type of recombination mechanism will be referred to as two-hole transfer transitions (THTT). However, it should be kept in mind that no exciton transfer occurs in the process, but instead part of the recombination energy is transferred to another acceptor during the recombination event. Further details on the interaction process producing these THTT spectra will

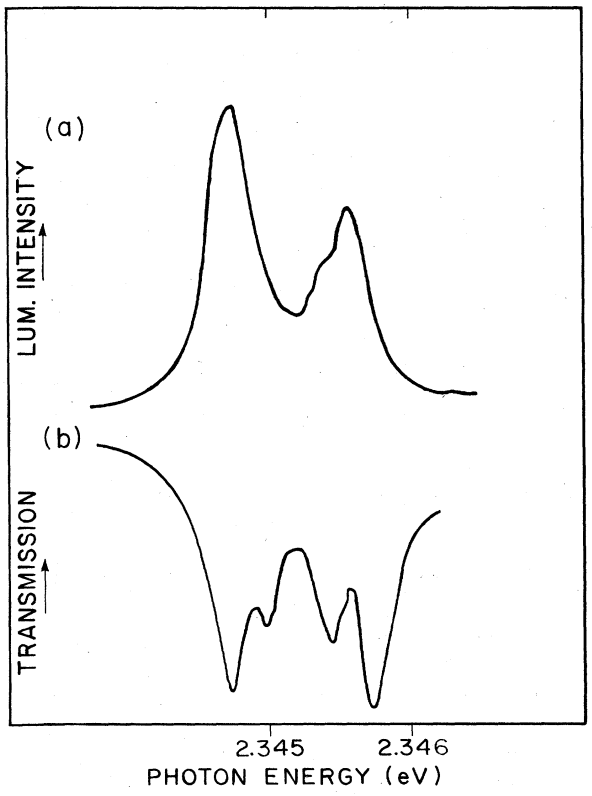

FIG. 5. Zeeman spectra for the Z_1^0 emission measured at 10 T in (a) luminescence (with $\mathbf{H}||\langle 110\rangle$) and (b) transmission (with $\mathbf{H}||\langle 111\rangle$). As observed, no thermalization occurs in absorption, in contrast to PL emission, where the thermalization effect is obvious. Such behavior is expected for isoelectronic centers, where no spin (i.e., no electronic particle) occurs in the ground state of the BE system.

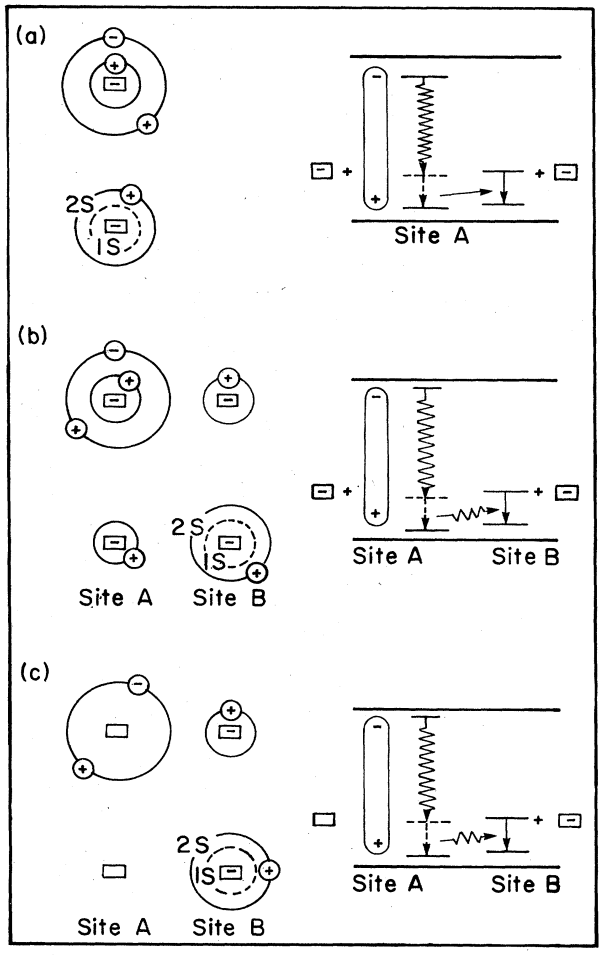

FIG. 6. (a) Illustration of the so-called two-hole transitions (THT's). When an exciton bound at an acceptor at site A recombines, part of the recombination energy is transferred to the hole of the acceptor, at which the exciton is bound. The BE recombination energy is therefore reduced by the amount corresponding to the energy required for excitation of the acceptor hole. (b) For a two-hole transfer transition (THTT) part of the BE recombination energy is instead transferred to a nearby acceptor at site B in contrast to "ordinary" THT, where the acceptor (site A) binding the exciton is excited. The detected recombination energy at a THTT process then corresponds to the BE energy reduced by the energy needed to excite the nearby acceptor. (c) THTT processes occur not only for excitons bound at acceptors [Fig. 6(b)], but also for excitons bound at isoelectronic centers, where "ordinary" THT's cannot occur. Two of the investigated BE centers (Z_1^0 and Z_2^0) for which transfer processes are observed are bound at complex isoelectronic centers, while the remaining BE's ($Z_3^0-Z_5^0$) are bound at complex acceptors.

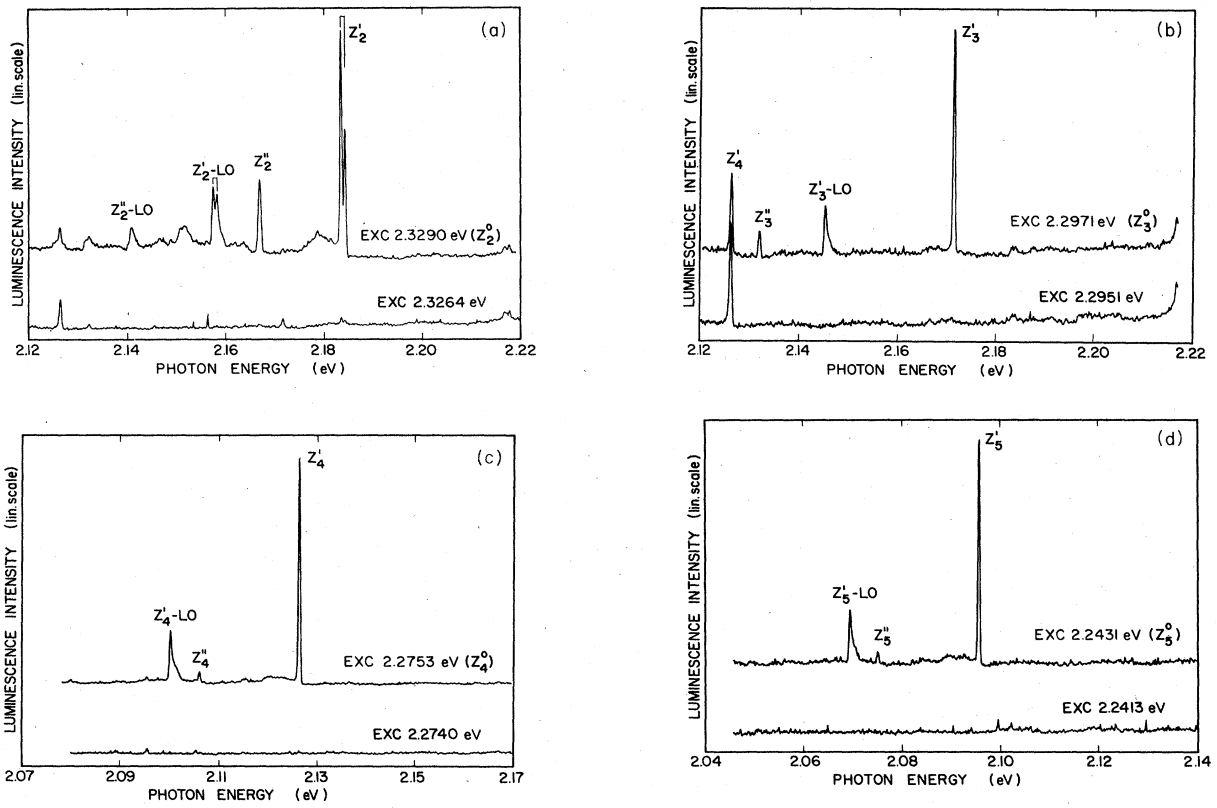

FIG. 7. Selective photoluminescence (SPL) spectra for the BE's Z_2^0–Z_5^0 corresponding to the SPL spectrum for Z_1^0 shown in Fig. 4. For all these centers two satellite lines are observed, e.g., Z_2' and Z_2''. (There is some uncertainty, however, whether Z_4'' and Z_5'' are THTT lines or phonon replicas of Z_4' and Z_5', respectively.)

be discussed in Sec. IV below.

In a similar way as for the Z_1^0 BE state, electronic satellite spectra are also observed for the other strong BE emissions Z_2–Z_5 shown in Fig. 1. The relevant SPL spectra for these centers are collected in Fig. 7. It is observed that for each center a different characteristic satellite spectrum is observed. The energies and intensity ratios of satellite lines relative to the principal electronic BE lines are collected in Table I. The strength of the satellite lines compared to the corresponding electronic line is rather strong in all cases, particularly for the deeper excitons Z_3–Z_5. It should be kept in mind, however, that for these high doping levels the overall PL intensity of the samples is reduced 2–3 orders of magnitude, compared to a low doped ZnTe sample. This is probably a manifestation of quite strong intersite Auger effects in the BE

TABLE I. Photon energies and intensity ratios for the satellite lines and corresponding parent BE lines.

Parent BE		Satellite line 1				Satellite line 2			
Notation	Photon energy (eV)	Notation	Photon energy (eV)	Energy displacement from parent BE (meV)	Intensity ratio to parent BE	Notation	Photon energy (eV)	Energy displacement from parent BE (meV)	Intensity ratio to parent BE
Z_1^0	2.3452	Z_1'	2.2507	94.5	0.11	Z_1''	2.2176	127.6	0.04
Z_2^0	2.3296	Z_2'	2.1844 2.1837	145.2 145.9	0.02 0.04	Z_2''	2.1670	162.6	0.01
Z_3^0	2.2980	Z_3'	2.1721	125.9	0.19	Z_3''	2.1327	165.3	0.02
Z_4^0	2.2761	Z_4'	2.1267	149.4	0.20	Z_4''	2.1065	169.6	0.01
Z_5^0	2.2443	Z_5'	2.0958	148.5	0.25	Z_5''	2.0754	168.9	0.01

recombination, whereby the entire BE energy is transferred to a hole ejected into the valence band from an interacting acceptor. From a comparison between PL and transmission spectra measured at high magnetic field it is concluded that Z_1 and Z_2 are excitons bound at isoelectronic complex defects (IBE's), while Z_3-Z_5 are bound to complex acceptors (ABE's).[8] The satellite lines related to the ABE's are generally stronger, as observed in Table I. PLE spectra for the satellite lines associated with the Z_2-Z_5 excitons are collected in Fig. 8, indicating that these lines are not real excitations. They are rather two-hole transitions (THT) or THTT states, similar to the Z_1' and Z_1'' lines described in more detail above (Figs. 2–5).

It is interesting to note from Fig. 7 and Table I that the Z_1-Z_5 BE's are usually associated with two electronic satellite lines. [There is some uncertainty as to whether Z_4'' and Z_5'' are electronic lines or just phonon replicas of Z_4' and Z_5', respectively, since the energy displacement (20.3 meV) is close to the energy of a gap mode commonly occurring in the spectra of these centers.[9]] Thus more than one acceptor is interacting with some BE states, and is subject to final-state excitation in the BE recombination.

For the ABE's (Z_3-Z_5) ordinary THT states may appear in contrast to the case of IBE's (Z_1 and Z_2). That possibility can therefore not be ruled out for one of the observed satellite lines related to each of the Z_3-Z_5 centers. However, at least some of the satellite lines related to Z_3-Z_5 are necessarily THTT states, e.g., the energies of Z_3' and Z_3'' are not consistent with ordinary THT states. Two alternative interpretations of the observed satellite lines are provided in Table II. In both cases four different acceptors seem to be important for the interaction with the $Z_1^0-Z_5^0$ BE states giving rise to THTT satellites. The perturbed $1s$-$2s$ acceptor excitation energies are 94.5 meV (acceptor 1), 125–128 meV (acceptor 2), 145–149 meV (acceptor 3), and 162–169 meV (acceptor 4). Table II shows that the transferred electronic energies differ between the BE states Z_1-Z_5, and thus appear to be selective for each initial BE state. It is also notable that in no case was any trace of a third THTT observed for Z_1-Z_5. There is a correlation (though not complete) between higher transfer energies and deeper BE states, i.e., a more efficient interaction with deep nearby acceptors for the deep BE's. In addition, for the BE states, which have the same final-state excitations, a slight difference in transferred energies can be noticed (e.g., $Z_1^0-Z_1''=127.6$ meV and $Z_3^0-Z_3'=125.9$ meV). These differences can vary from 1 meV up to several meV between different principal BE states (Table I). A discussion on the possible

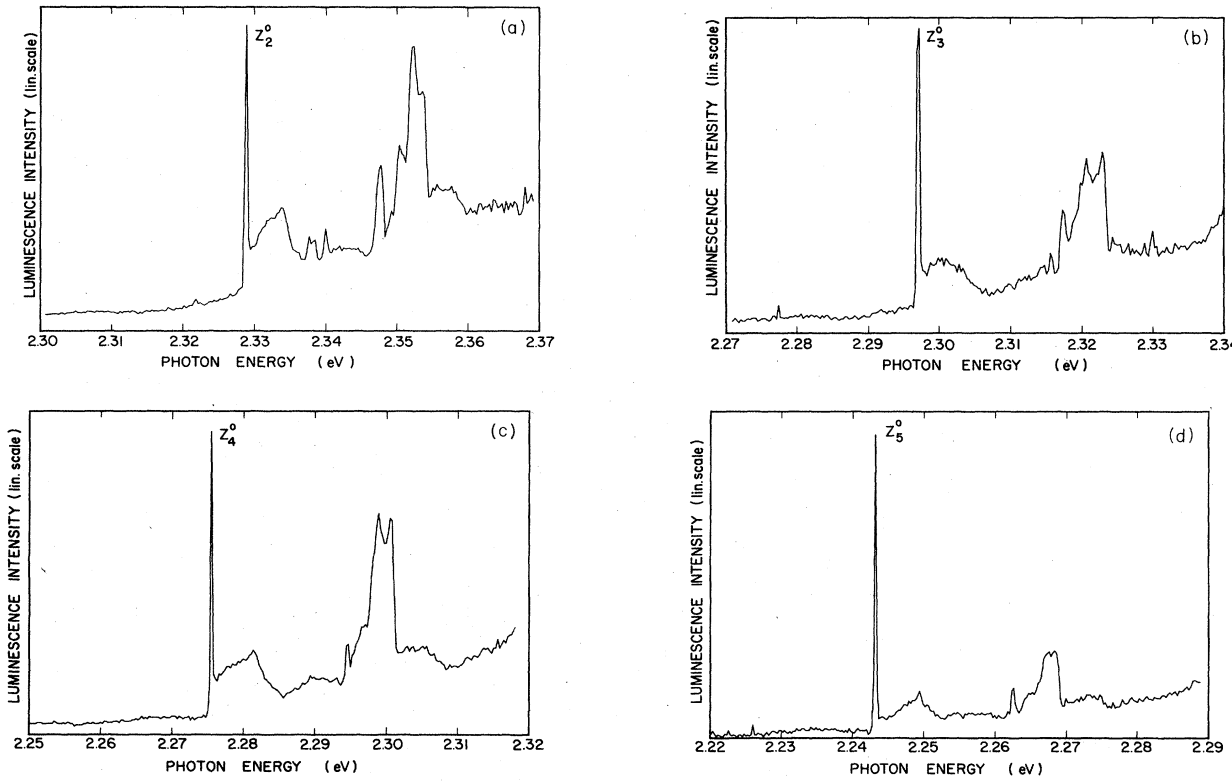

FIG. 8. PLE spectra for the emissions $Z_2^0-Z_5^0$, where the detection in all cases is in the first satellite line $Z_2'-Z_5'$ [thus corresponding to Fig. 3(c) for the Z_1^0 emission]. All the PLE spectra are similar with a strong phonon sideband, particularly striking for the more shallow BE's. The phonon-coupling strength is considerably stronger than in the corresponding luminescence spectra.

TABLE II. Two alternative interpretations of the observed satellite lines. The interpretation involves THTT's to four different acceptors in the energy ranges 94.5 meV (acceptor 1), 125—128 meV (acceptor 2), 145—149 meV (acceptor 3), and 162—169 meV (acceptor 4). (acc. in table denotes acceptor, LOC denotes quasilocalized phonon mode.)

Satellite state	Z_1'	Z_1''	Z_2'	Z_2''	Z_3'	Z_3''	Z_4'	Z_4''	Z_5'	Z_5''
Energy displacement from parent BE (meV)	94.5	127.6	145.2 [145.9]	162.6	125.9	165.3	149.4	169.6	148.5	168.9
Interpretation I	THTT (acc. 1)	THTT (acc. 2)	THTT (acc. 3)	THTT (acc. 4)	THTT (acc. 2)	THTT (acc. 4)	THTT (acc. 3)	THTT (acc. 4) or Z_4' + LOC	THTT (acc. 3)	THTT (acc. 4) or Z_5' + LOC
Interpretation II	THTT (acc. 1)	THTT (acc. 2)	THTT (acc. 3, Z_4)	THTT (acc. 4, Z_3)	THTT (acc. 2)	THT	THT	THTT (acc. 4) or Z_4' + LOC	THTT (acc. 3, Z_4) or THT	THTT (acc. 4) or Z_5' + LOC

reasons for these variations will be reserved for Sec. IV.

Another possible THT mechanism not discussed here is, in principle, possible for complex acceptors which may have additional excited $1s$ hole states in the band gap due to the local strain field, which splits the bound hole states associated with the valence-band top. Such states are fundamentally different from the orbitally excited hole states associated with the ground state of the acceptor hole. It cannot be ruled out that such THT lines could be associated with some observed acceptor satellite lines in this case. Of course, such THT lines are not possible for IBE's, where no particles are available in the final state.

From a detailed study of the BE states and associated THTT lines at different temperatures, it is concluded that the intensity ratio between the principal BE lines in PL and the THTT satellites is almost independent of temperature, as exemplified for Z_1 in Fig. 9 and Table III. Similarly, they follow each other in intensity, when the excitation power is varied (Fig. 10 and Table IV). This behavior might be expected for electronic satellites, which are associated with the principal BE line. On the other hand, the intensity ratios between different principal BE lines in PL emission can vary with temperature (Table III), and particularly with the excitation power as shown in Fig. 10 and Table IV. This means that the total BE capture and recombination rates may change differently with these external parameters for each defect BE.

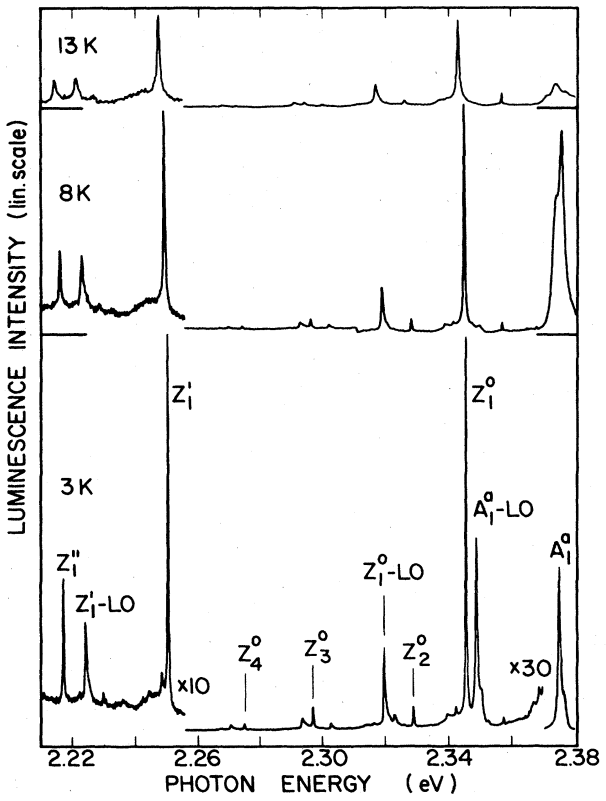

FIG. 9. PL spectra for Cu-doped ZnTe measured with band-gap excitation at some different temperatures. The intensity of the investigated emissions Z_1^0—Z_5^0 decreases quite rapidly to disappear at a temperature of ~20 K. The intensity ratios between these emissions can vary with temperature, which is accounted for in Table III. The intensity ratios between the satellite lines and corresponding principal BE lines is almost unaltered at different temperatures (see also Table III).

B. Resonant Raman scattering for Cu complex BE states

An important observation is that the same THTT satellite lines as observed in PL in the preceding subsection appear in Raman scattering. The Raman process dominates the PL spectrum for dye-laser excitation close to resonance with the principal BE line (Fig. 11). The Raman lines are easily distinguished from PL emission simply by their shift with the excitation energy, while the PL emis-

TABLE III. Intensity ratios for some satellite lines and parent BE lines at elevated temperatures.

Temperature (K)	Z_1^0	$\frac{Z_1'}{Z_1^0}$	$\frac{Z_1''}{Z_1^0}$	$\frac{Z_2^0}{Z_1^0}$	$\frac{Z_3^0}{Z_1^0}$
2	1.00	0.11	0.036	0.051	0.064
3	0.96	0.10	0.032	0.050	0.057
4	0.70	0.10	0.028	0.047	0.039
6	0.63	0.08	0.027	0.047	0.039
8	0.55	0.09	0.033	0.055	0.040
10	0.41	0.09	0.027	0.050	0.035
13	0.23	0.10	0.023	0.050	0.036
16	0.08	0.08		0.061	0.039

sion is stationary in energy, i.e., tied to the principal BE lines (Fig. 11). The Raman scattering efficiency for the two satellite lines Z_1' and Z_1'' is plotted in Fig. 12 as a function of the excitation energy in the region close to Z_1^0. As observed in Fig. 12, a marked threshold, particularly for Z_1'', appears in the RRS efficiency close to 2.343 eV. This energy coincides with the energy position of another BE emission observed in, e.g., the PL spectrum shown in Fig. 1. Thus the investigated scattering process occurs although considerably weakened for other centers than Z_1–Z_5. The resonances around Z_1^0 are somewhat broadened compared with the natural linewidths of the Z_1^0 BE line. This broadening is an intrinsic property of the Raman scattering process itself.[10]

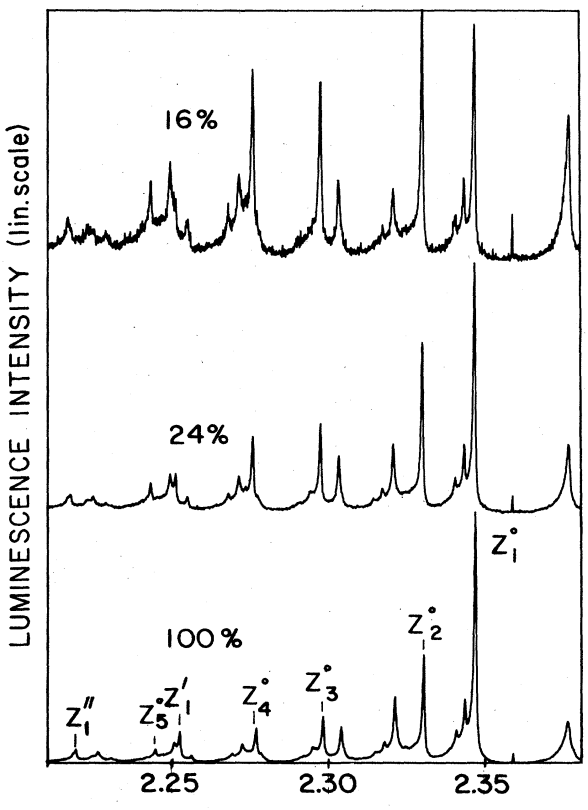

FIG. 10. PL spectra at 2 K for heavily-Cu-doped ZnTe, when the excitation power is varied. The intensity ratios between the deeper and shallower BE lines among the investigated Z_1^0–Z_5^0 emissions increase as the intensity of the band-gap excitation is reduced (see also Table IV).

The most important conclusion from the RRS data is that the scattering energies are exactly the same as the energy shifts for the satellites in PL spectra. Selection rules for RRS spectra strongly favor transitions between states of the same parity, i.e., the results support the assumption that the transfer energies in the THTT processes correspond to perturbed $1s$-$2s$ excitations in the final acceptor state.

Electronic Raman scattering has been observed before for BE centers in Cu-doped ZnTe, but in that case the detected transition originated from $1s$-$2s$ excitations of the acceptor binding the exciton,[11] in contrast to the case described here.

C. Magneto-optical properties of the THTT lines

In a Zeeman spectrum of a BE transition, the observed splittings reflect the behavior of both initial and final electronic states in a magnetic field. For a THTT, such as Z_1' or Z_1'' associated with the IBE state Z_1^0, the magneto-optical properties of the initial state should be identical to those of Z_1^0, while the final state should split as an acceptor hole state. This could give rise to quite complicated Zeeman spectra, which are also found in experiments for Z_1' and Z_1''. Figure 13 shows Zeeman splitting at 10 T in PL of the three lines Z_1^0, Z_1', and Z_1'' for the same crystal orientation versus the magnetic field. The IBE Z_1^0 shows some thermalization in the initial state (the excited state of the BE system), as expected. The thermalization in the initial BE state can also be observed to some extent in the Zeeman data for Z_1' and Z_1'', although partly disguised by a complicated structure.

The Zeeman spectrum of Z_1', shown in Fig. 13(b), is considerably more complex and, in addition, much broader than the corresponding Zeeman spectrum of Z_1'' [Fig. 13(c)]. Such a complex spectrum is expected for the case of a transfer transition to an axial acceptor (the final state). Each particular line cannot be identified without knowledge of the shallow acceptor responsible for Z_1'. If the acceptor is assumed to be axial with an axis different from the axial center binding the principal BE Z_1^0, a large

TABLE IV. Intensity ratios for some satellite lines and parent BE lines at different excitation intensities.

Excitation intensity	$\frac{Z_1'}{Z_1^0}$	$\frac{Z_1''}{Z_1^0}$	$\frac{Z_2^0}{Z_1^0}$	$\frac{Z_3^0}{Z_1^0}$	$\frac{Z_4^0}{Z_1^0}$	$\frac{Z_5^0}{Z_1^0}$
1.00	0.11	0.04	0.40	0.15	0.13	0.03
0.24	0.12	0.05	0.66	0.31	0.29	0.07
0.16	0.12	0.11	1.04	0.67	0.77	0.19

number of inequivalent defect configurations relative to the magnetic field direction occur both for the initial and final states. The number of different axes at different sites is in a general direction multiplicative in determining the total number of possible lines. If the principal number of lines N for Z_1' is 8 [Fig. 13(b)], this number has to be multiplied by a factor N_A to take into account the number of possible inequivalent orientations of the Z_1^0 defects at site A for the initial state, and also multiplied by a similar factor N_B for the final-state axial acceptor at site B, which has a different axis. For the initial state, the factor N_A should be 4, since we have four trigonal defect axes. The symmetry of the final-state axial acceptor responsible for Z_1' is not known and therefore N_B could be larger than 4. Evidently, for a general direction of magnetic field, at least 128 lines are expected in a Zeeman spectrum (if selection rules are not taken into account), causing the complexity of the Z_1' spectrum. A detailed analysis of each line of the spectrum is impossible unless much higher fields are used to resolve the lines clearly.

A notable observation from the Zeeman spectrum of Z_1' is its extensive width compared with the corresponding spectra for Z_1^0 and Z_1'' (Fig. 13). This is interpreted in terms of a quite large effective g value, g_{eff}, for the hole of the axial acceptor in the final state. Again, without an identification of each individual line in the spectrum, a value of g_{eff} for the hole in the final state cannot be determined. A rough estimate from the width of the Zeeman spectrum as composed of a superposition of the Zeeman spectra for the Z_1^0 state and the hole in the final state [Figs. 13(a) and 13(b)] gives an effective splitting of the final state of about 1.5 meV at 10 T, corresponding to a g_{eff} value of about 2.7, i.e., $K \approx 0.9$.

For the case of Z_1'', a simpler picture is obtained in the Zeeman spectrum. This can be understood if the final-state acceptor is assumed to be the substitutional Cu_{Zn} acceptor. In this case there are four different Zeeman-split hole states, since the axial field splitting of hole states is absent in this case. The main simplification in this case is that we have a tetrahedral crystal field on site B, which

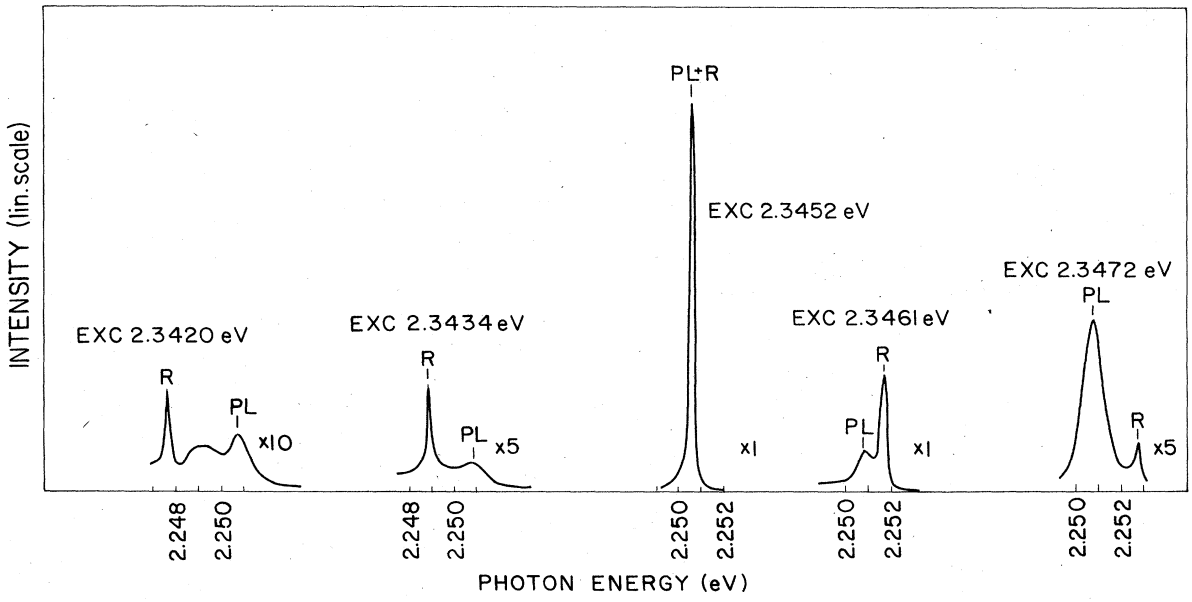

FIG. 11. Resonant Raman scattering (RRS) for the Z_1^0 BE close to the Z_1' PL satellite. At selective excitation resonant with Z_1^0, the intensity of Z_1' at 2.2507 eV (94.5 meV below Z_1^0) reaches its maximum (the spectrum in the middle of the figure). When the selective excitation is slightly shifted in one direction or the other, a second peak appears besides the ordinary Z_1' PL line at 2.2507 eV. This second peak, the Raman component, is always displaced 94.5 meV from the excitation energy. The Raman peak is easily observed for excitation energies in the range ±6 meV from Z_1^0. A RRS spectrum derived in this way is shown in Fig. 12.

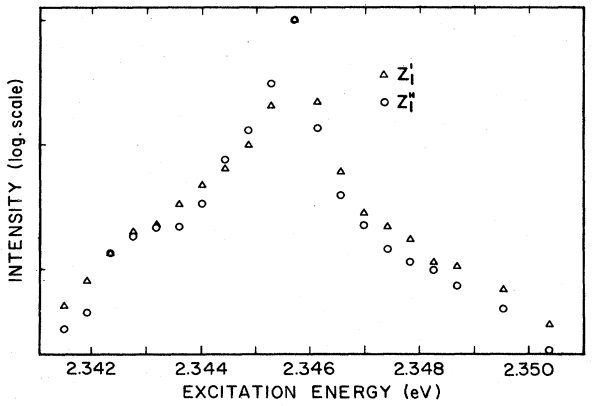

FIG. 12. The efficiency of the Raman scattering for the satellite lines Z_1' and Z_1'' as a function of the excitation energy close to Z_1^0. The efficiency for the two scattering processes are normalized at the maximum (excitation resonant with Z_1^0). A shoulder in the spectrum (particularly for Z_1'') can be observed at ~2.343 eV corresponding to the position of another acceptor-related BE (Fig. 1).

means that the splitting of the hole in the final state is approximately isotropic. We therefore expect a maximum of $4\times4=16$ different Zeeman-split lines in the spectrum of Z_1'', much less than for Z_1'. Even though these lines are not resolved in Fig. 13(c) at 10 T, the suggested multiplicity appears plausible from the spectrum. The width of the Z_1'' Zeeman spectrum is also consistent with the combined widths of Z_1^0 and the Cu_{Zn} acceptor previously studied.[11]

D. Phonon interaction in THTT spectra

The phonon spectrum associated with a THTT line is different from what is observed for the principal BE in the PL spectrum (which, in turn, may differ strikingly from the absorption spectrum for the BE; see, e.g., Figs. 7 and 8). The LO—phonon coupling dominates strongly for both the principal BE and the THTT lines, but weaker coupling to the entire ZnTe phonon spectrum is also observed. In addition, defect-induced quasilocalized modes as well as gap modes occur at resonant excitation in the no-phonon line, as shown in Fig. 14 for Z_1^0–Z_5^0. A comparison between the phonon spectra associated with the principal BE states and the corresponding phonon spectra for their satellite lines shown in Fig. 15 reveals that the phonon coupling to these satellite lines is generally stronger than for the principal BE lines (with the exception of LO_Γ, which has a similar coupling strength). In addition, different quasilocalized modes appear in the BE phonon spectra than in the corresponding THTT spectra. The general difference in phonon-coupling strength between the BE spectra and THTT spectra is analogous to the case observed in ordinary two-hole spectra for shallow acceptors. For instance, the phonon coupling associated with a THT is considerably stronger than the corresponding coupling for the principal ABE related to the simple substitutional Cu_{Zn} acceptor.[7]

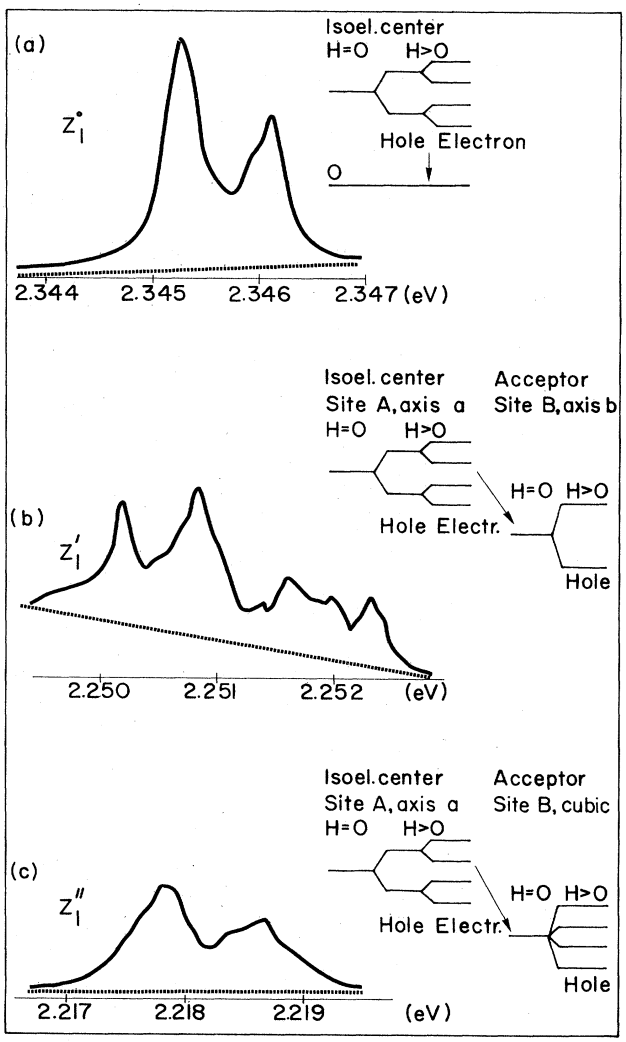

FIG. 13. Zeeman splittings for Z_1^0, Z_1', and Z_1'' measured at the same crystal orientation in a magnetic field of 10 T in PL. (a) The detected Zeeman spectrum for Z_1^0 in the left-hand part of the figure. As is shown elsewhere (Ref. 8), the exciton giving rise to the Z_1^0 emission is bound at an isoelectronic defect. A schematic representation of the electron-hole coupling, which gives rise to the observed spectrum, is also shown. (b) Zeeman splitting of the Z_1' line. This spectrum is considerably broader and more complex than Z_1^0 in (a). The completely different spectrum compared to Z_1^0 is explained by a THTT process involving a nearby acceptor at site *B*. This acceptor is assumed to be axial with its axis in a direction other than Z_1^0. (c) Zeeman spectrum for the Z_1'' line. This spectrum is less complex than the corresponding spectrum for Z_1'. The simpler behavior for Z_1'' is accounted for by the assumption that the final-state acceptor is a single, substitutional acceptor (Cu_{Zn}) with an approximately isotropic hole splitting.

The enhancement of the coupling strength is even more striking in excitation spectra of the principal Z_1^0 BE, where a strong phonon sideband in the acoustic range is observed.

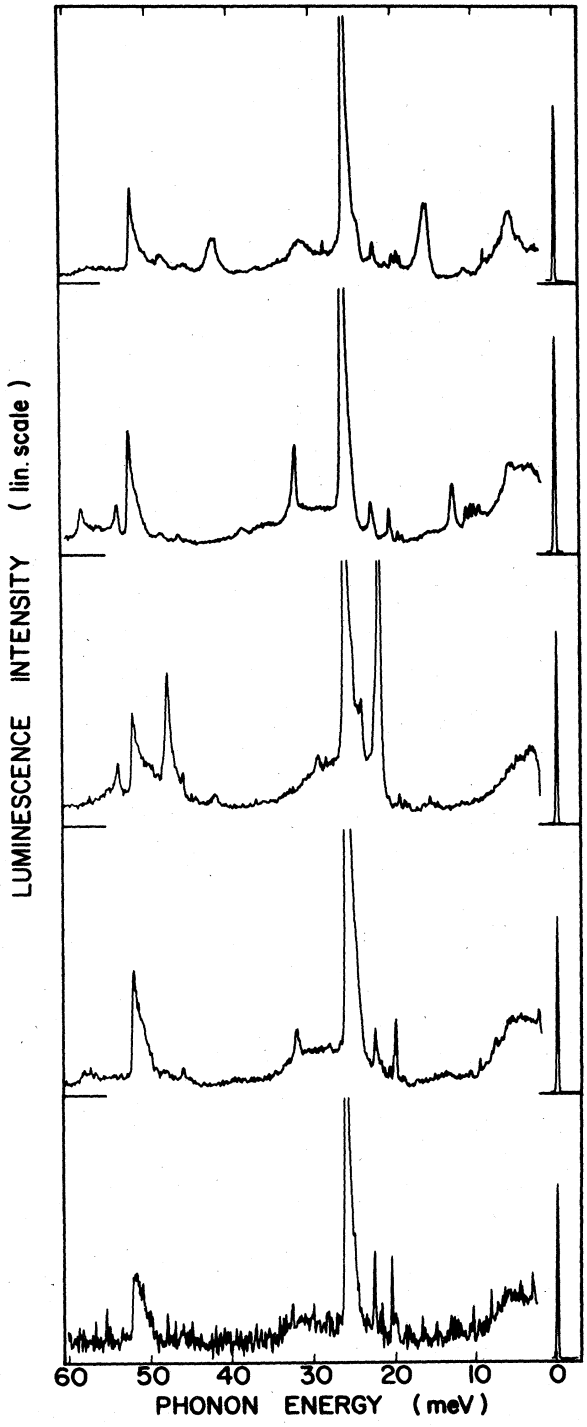

FIG. 14. Phonon sidebands in PL for the principal BE's $Z_1^0-Z_5^0$. The phonon-assisted spectrum for Z_1^0 shown in the topmost part, for Z_2^0 below, and so on. In addition to the strongest LO mode at ~26 meV, weaker defect-induced gap modes and quasilocalized modes in the acoustic- as well as the optical-phonon branches occur.

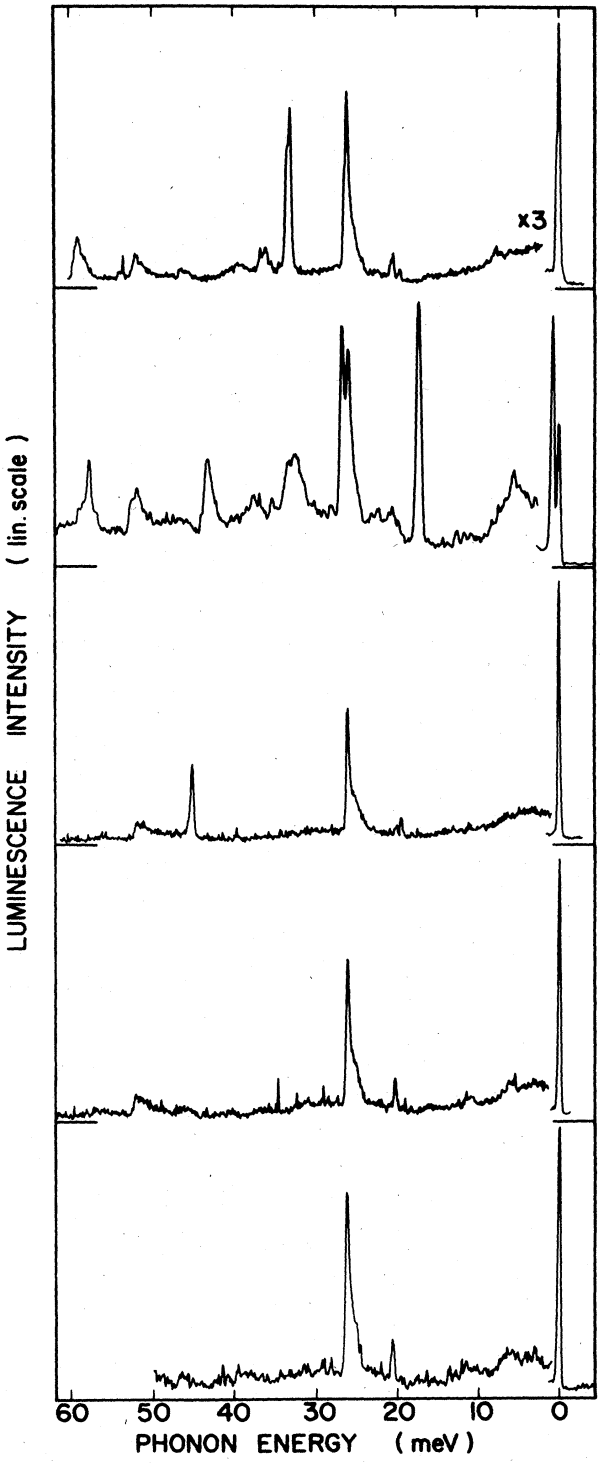

FIG. 15. Phonon sidebands for the satellite lines $Z_1'-Z_5'$ measured in PL (Z_1' topmost, Z_2' below, and so on). These spectra should be compared with the corresponding phonon sidebands for the principal BE's in Fig. 14. As observed, the phonon coupling is generally stronger for these satellite lines than for the corresponding principal BE's (with the exception of the LO_Γ replica). Also, the gap and quasilocalized modes appear at energy positions other than those observed in the phonon sidebands for the principal BE's.

Since also a THT or THTT involves an excitation process, the same mechanism as in excitation measurements is assumed to be responsible for the increased phonon-coupling strength. The considerable enhancement of phonon coupling in absorption compared to emission, which occurs for the $Z_1^0-Z_5^0$ BE states, is discussed separately.[9] A strong interaction between pure electronic and phonon-assisted transitions is concluded to give rise to the strong phonon coupling in absorption. A similar action could be responsible for the difference in coupling strength between BE spectra and THT or THTT spectra.

IV. DISCUSSION

A. Schematic model of two-hole transfer transitions

Any bound-exciton excitation should, in principle, be treated as a many-body electronic problem even without intersite interaction, as manifested by the early observations of two-particle spectra for donor-bound-exciton (DBE) or ABE recombination. Similar satellite spectra are seen in photoelectron excitations in atomic systems where many electrons are affected in a single photoexcitation event, in addition to the primarily excited particle.[12] Relative intensities of such satellites in atomic spectra are also similar to what is seen with bound excitons in semiconductors, i.e., typically a few percent or less of the principal transition strength. In this paper we have described the corresponding additional possibilities with BE recombination in interacting systems, where site transfer of excitation can partly occur. The discussion of these processes will be only schematic, since a proper treatment of transitions within an interacting many-particle system is obviously quite complicated.

If we consider the situation described in Fig. 6, the initial state in a THTT process, involving for simplicity an IBE, can be represented by a wave function of the type

$$|i\rangle = G_0(\mathbf{r}_{h1},\mathbf{r}_e,\mathbf{R}_1)H_{1s}(\mathbf{r}_{h2},\mathbf{R}_2) ,$$

i.e., it contains a wave function for the electron e and hole h_1 (BE excitation) bound at site $\mathbf{R}_1$ and, in addition, a hole h_2 in its ground state (lowest $1s$ orbital state) on a neutral acceptor at site $\mathbf{R}_2$. Similarly, the final state in a THTT can be expressed as

$$|f\rangle = G'(\mathbf{R}_1)H_{2s}(\mathbf{r}_{h2},\mathbf{R}_2) ,$$

where $G'(\mathbf{R}_1)$ denotes the fact that at $\mathbf{R}_1$ no electronic particle is now present, while at site $\mathbf{R}_2$ an excitation of the hole into a $2s$ excited orbital state has occurred. The total wave function of the initial state is quite complex in practice due to correlations between the particles involved, and it can only be treated in a simple approximate way in cases where one of the particles is very loosely bound compared to the other (the HTL model[13]). For the case of an ABE in the initial state, the situation is even more complex, since three interacting electronic particles are involved at site $\mathbf{R}_1$. It is not possible to obtain, in general, an analytical expression for the BE wave function without drastic approximations. Even for the simpler IBE case we have totally three interacting particles at two sites. A Hartree-Fock scheme can be used to treat the exchange problem,[14] but it is complicated here by the fact that two sites are involved. To take correlations into account it is possible to employ a scheme of configuration interaction,[15] where the wave functions of the bound excitons are expanded in Slater determinants. The basic functions then include spatially symmetric combinations of single-particle orbitals. Such models have been valuable for calculations of correlation effects of donor-acceptor pairs,[16] a problem which has similarities with the interacting systems investigated in this report. The initial- and final-state wave functions can then be developed in these basic functions.

The transition matrix elements for THTT lines should be of the general form

$$M \approx \langle i | P | f \rangle ,$$

where P is the conventional dipole operator in optical transitions, and $|i\rangle$ and $|f\rangle$ are given by the above expressions. If the coefficients in the development of the initial-state wave functions in the basic functions are nonzero, the transition matrix elements to excited final-state configurations will also be nonzero. For transitions with sufficiently large matrix elements, detectable THTT states are provided in the PL spectra. The above discussion is analogous to the case of ordinary two-hole spectra, with the important difference that in the THTT case two distinct lattice sites are involved.

Since the interacting Coulomb potential is an even function in space, a perturbation expansion of the coefficients in a configuration expression of the initial state restricts the nonzero transition matrix elements[17]

$$\langle f_{1s}^{h_1} | f_{nl}^{h_2} \rangle$$

to even-parity transitions in the case of ordinary two-hole transitions (THT), i.e., only $1s$-$2s$, $1s$-$3s$, etc. types of final-state excitations are observed.[2] In the THTT case the main difference with the THT problem is that two different sites are involved in the initial and final states. This means that some overlap integrals of the type

$$\langle f^{h_1}(\mathbf{r}_1) | f^{h_2}(\mathbf{r}_2) \rangle$$

in the THT case are exchanged for

$$\langle f^{h_1}(\mathbf{r}_1,\mathbf{R}_1) | f^{h_2}(\mathbf{r}_2,\mathbf{R}_2) \rangle$$

in the case of a THTT matrix element. A term, which includes the wave-function overlap of the type $\exp[-\alpha(R_1-R_2)]$, is introduced in the transition probability, which will affect the strength of the transitions. The selection rule could be relaxed due to the reduced symmetry, when two sites are involved, as observed for, e.g., pair transitions. However, the conclusion from the SPL and RRS experiments described in the preceding sections is that only transitions to even-parity states are observed, which indicates an insignificant relaxation from the selection rules valid for THT.

B. Satellite transition energies

An important point in the model discussed here as an explanation for the observed THTT lines for $1s$-$2s$ excitations in the final state of acceptors interacting with the initial-state BE is the identification of these final-state ac-

ceptors. Apparently, several different final-state acceptors must be present according to Table I, the shallowest one with $1s$-$2s$ energy at about 94.5 meV and further at ≈ 128 meV and so on. As was discussed above in Sec. III C, the magneto-optical data support the idea that the former one (i.e., the Z_1' line) corresponds to a complex shallow acceptor in the final state, which we tentatively identify with the previously observed so-called k acceptor with an unperturbed $1s$-$2s$ hole-energy difference of 93 meV.[18] Similarly, the Z_1'' line (at 127.6 meV) is believed to correspond to a $1s$-$2s$ excitation at substitutional Cu_{Zn} acceptors [the unperturbed $1s$-$2s$ transition 125.1 meV (Ref. 7)]. This identification is also supported by the magneto-optical data (Sec. III C). Fourier-transform infrared- (FTIR) absorption measurements on the same sample showed notable lines originating from transitions of the Cu acceptor, while corresponding lines from k-acceptor transitions were much weaker (probably due to the position of the Fermi level in the sample). The higher THTT transfer energies in Table I are believed to be associated with somewhat deeper unidentified acceptors in a similar way. A minor discrepancy is that the final-state excitation energies in this model are slightly shifted from what is observed for unperturbed acceptor states at low doping. The difference is about 1.5 meV for Z_1' and 2 meV for Z_1''; possibly even larger for the lower-energy THTT lines. The search for the explanation of this shift in energy is complicated by the linewidth of the THTT satellites, which is as narrow as observed for the initial BE's (0.3—0.5 meV).

Final-state excitations for the k acceptor are observed in just one case (Z_1'). Transfer transitions connected with the Cu_{Zn} acceptor, on the other hand, are observed for both the Z_1 and the deeper Z_3 centers, and this transition constitutes the most thoroughly investigated case among the THTT's, where the same initial state BE is related to more than one final-state acceptor via transfer processes. Furthermore, the transitions involving the acceptor are interesting also from another aspect, namely that the initial state is in one case an exciton bound at an isoelectronic center (Z_1) and in the other at an acceptor (Z_3). The energy difference $Z_3^0 - Z_3'$ is almost the same as observed in ordinary THT for the Cu ABE, while the energy of $Z_1^0 - Z_1''$ exceeds the $1s$-$2s$ excitation of the unperturbed Cu acceptor by ≈ 2 meV. General trends for the spread of transfer transition energies (Tables I and II) depending on different parameters (e.g., the exciton binding energy, acceptor, or isoelectronic center as the initial state) are, however, difficult to establish from the present collection of data. This discussion will therefore only touch upon some possible origins of the observed spread in transfer energies. Since the value on the transition energy is an energy difference, the perturbation may originate from either the initial state or the final state in the optical transition, or both.

If the $1s$-$2s$ discrepancy originates from the initial state, the inhomogeneous distribution of complex defects in the Cu-doped material can be the reason for these effects. Such inhomogeneities have been demonstrated previously by topographic studies of cathodoluminescence on similar Cu-diffused material.[19] The occurrence of the THTT satellites as well as the principal BE states are concentrated around the Te-rich inclusions always present in the bulk ZnTe. The strong increase in concentration of various Cu-related complex defects close to these inclusions may cause an increase of the binding energies for the $1s$ ground state of the interacting acceptor binding the exciton in the initial state due to a simple addition of contributions from hole-attractive defect potentials.

If, instead, the discrepancy of the $1s$-$2s$ energy occurs in the final state, the interaction between the final $2s$ state of the hole of the nearby acceptor and the complex defect potential originally binding the exciton (i.e., before the recombination event) must be considered. This interaction is assumed to be of a quite different nature, depending on whether the potential originates from an acceptor or an isoelectronic center. Various types of Coulomb interaction terms could give rise to perturbation of the $2s$ hole state. (The potential originating from the isoelectronic center is then assumed to be polarized.) Overlap of final-state hole wave functions and configuration interaction (for the acceptor BE case) are other possible sources for a distorted $2s$ hole state, i.e., the same type of interaction as used to calculate correction terms to the simple Coulomb expression for close pairs.[16]

From the data available at the present stage we cannot conclude whether the observed small discrepancies in transfer energy originate from the initial or final state, or possibly from both. The combination of these perturbations could be the reason for the observed irregularities in the transfer transition energies for different initial-state BE's. Indeed, we are dealing with a many-particle problem, and any model based on corrections in a single-particle energy scheme may be too simplified. For a complete description many complications have to be solved, e.g., the linewidth, which is of the same order as for ordinary THT lines.

C. Specific properties of THTT lines

An important difference between the THT and THTT problem is that the two different sites involved in the latter case make the spatial extent of the wave functions of the initial-state BE particles very important for the strength of possible THTT lines. In the cases studied here the initial BE's Z_1^0—Z_5^0 are all of a rather simple type with a loosely bound electron, as is evident from magneto-optical Zeeman data published separately.[8] This means that the electron binding energy in the initial BE state is of the order 15—20 meV, and the electron wave-function envelope f^e is quite extended. Therefore matrix elements of the type

$$\langle f^e(\mathbf{r}_1,\mathbf{R}_1) \,|\, f^{h_2}(\mathbf{r}_2,\mathbf{R}_2)\rangle$$

are quite important in determining the strength of the THTT lines, since here the overlap between initial and final states is considerable. The overlap with the final-state wave function is larger in the excited $2s$ hole state at $\mathbf{R}_2$ than with the ground state of the acceptor, in contrast with ordinary THT, where the overlap with the $1s$ hole state is the dominating term, since the involved particles are localized on the same site.

The high doping level makes screening important for the higher excited acceptor states, which means that they are not distinguished as discrete states in final-state interactions of the THTT type. Exactly the same phenomenon is also observed for ordinary THT spectra, which are found to disappear at sufficiently high doping levels, due to screening of the corresponding excited hole state wave functions. An interesting aspect of this screening mechanism is that the THTT lines are observed even though the ordinary THT lines for Cu_{Zn} have almost disappeared. Apparently the THTT lines survive to a somewhat higher doping level, although the THT and THTT lines can coexist with similar strength at a suitable doping level. A definite explanation for this behavior cannot be provided from the present schematic analysis.

Another specific property (without any obvious explanation) is the apparently selective coupling between the BE initial state and the acceptors in the final state. For none of the BE states are transfer transitions involving more than two final-state acceptors observed; not even a trace of a third satellite state can be detected. For this selective coupling there is a connection, although not unambiguous, between the binding energy of the BE state and the acceptor involved in the transfer transition. Transfer processes occur preferably for shallow BE states and shallow acceptors, while deep BE's connect to deep acceptors.

V. CONCLUSIONS

In this paper satellite spectra in bound-exciton recombination in ZnTe are reported, involving interaction between the bound exciton and an acceptor at some considerable distance (hundreds of Å) at high doping levels. The recombination process appears to be dominated by impurity Auger effects, where holes at acceptor sites are ejected into the valence band upon bound-exciton recombination, causing a dominating nonradiative channel. The radiative part shows satellite spectra associated with bound-exciton recombination; the satellite lines have an intensity of typically several percent of the corresponding bound-exciton line and are down-shifted in energy by approximately the $1s$-$2s$ excitation energy of the interacting shallow acceptors. The same satellite transitions occur in resonant Raman scattering. In addition, it appears to be effective for both neutral isoelectronic bound excitons and such associated with acceptors.

In this first report of such satellite lines, here denoted two-hole transfer transitions (THTT's), as distinguished from the ordinary one-site two-hole transitions (THT's), we believe that the basic model of these satellites has been established from rather careful studies of optical spectra such as photoluminescence, excitation spectra, transmission, resonant Raman scattering, and Zeeman spectra.

Certainly several details in the recombination process, such as the minor energy shifts observed in these satellites compared to unperturbed $1s$-$2s$ acceptor energies and the surprisingly small linewidth of the satellite lines, remain to be studied in more detail later. In addition, it should be of interest to prepare similar defect systems in highly doped semiconductors other than ZnTe, which has so far not been done.

ACKNOWLEDGMENTS

One of us (B.M.) is deeply grateful for financial support from Université Scientifique et Medicale de Grenoble (USMG) and from Centre d'Etudes de Nucléaires Grenoble (CENG) during a sabbatical period. In addition, we are indebted to L. Revoil and S. Jeppesen for valuable assistance in sample preparation.

[1]M. Lampert, Phys. Rev. Lett. **1**, 450 (1958); J. R. Haynes, *ibid.* **4**, 361 (1960).

[2]P. J. Dean and D. C. Herbert, *Excitons,* Vol. 14 of *Topics in Current Physics,* edited by K. Cho (Springer, Berlin, 1979), p. 55.

[3]E. Cohen and M. D. Sturge, Phys. Rev. B **15**, 1039 (1977).

[4]H. P. Gislason, B. Monemar, P. J. Dean, and D. C. Herbert, Physica **117&118B**, 269 (1983).

[5]D. Labrie, T. Timusk, and M. L. W. Thewalt, Phys. Rev. Lett. **52**, 81 (1984).

[6]P. J. Dean, J. D. Cuthbert, D. G. Thomas, and R. T. Lynch, Phys. Rev. Lett. **18**, 122 (1967).

[7]N. Magnea, D. Bensahel, J. L. Pautrat, and J. C. Pfister, Phys. Status Solidi B **94**, 627 (1979).

[8]B. Monemar, P. O. Holtz, H. P. Gislason, N. Magnea (unpublished).

[9]P. O. Holtz and B. Monemar (unpublished).

[10]R. M. Martin and L. M. Falicov, *Light Scattering in Solids,* Vol. 8 of *Topics in Applied Physics,* edited by M. Cardona (Springer, Berlin, 1975), p. 80.

[11]P. J. Dean, H. Venghaus, J. C. Pfister, B. Schaub, and J. Marine, J. Lumin. **16**, 363 (1978).

[12]G. Wendin, in *X-Ray and Atomic Inner-Shell Physics—1982 (University of Oregon),* proceedings of the International Conference, edited by Bernd Crassman (AIP, New York, 1982), p. 495.

[13]J. J. Hopfield, D. G. Thomas, and R. T. Lynch, Phys. Rev. Lett. **17**, 312 (1966).

[14]A. M. Stoneham and A. H. Harker, J. Phys. C **8**, 1102 (1975).

[15]D. C. Herbert, J. Phys. C **10**, 3327 (1977).

[16]L. Mehrkam and F. Williams, Phys. Rev. B **10**, 3753 (1972).

[17]N. Magnea, these d'Etat, Université Scientifique et Medicale de Grenoble, Grenoble, 1982.

[18]H. Venghaus and P. J. Dean, Phys. Rev. B **21**, 1596 (1980).

[19]D. Bensahel, N. Magnea, and M. Dupuy, Solid State Commun. **30**, 467 (1979).